Advances and Applications in Mechanical Engineering and Technology
Volume 5, Number 1, 2014, Pages 1-26

NUMERICAL SIMULATION OF SLOSHING PROBLEM IN RECTANGULAR TANK

N. COULIBALY[1], M. DOSSO[2] and E. DANHO[1]

[1]Laboratoire de Mécanique
UFR Mathématiques-Informatique
Université Félix Houphouët
Abidjan-Cocody 22 BP 582 Abidjan 22
Côte d'Ivoire
e-mail: coulnamson@hotmail.com
danhoemile@yahoo.com

[2]Laboratoire de Mathématiques Appliquées
UFR Mathématiques-Informatique
Université Félix Houphouët
Abidjan-Cocody 22 BP 582 Abidjan 22
Côte d'Ivoire
e-mail: mouhamadou.dosso@univ-fhb.edu.ci

Abstract

This paper presents a volume of fluid (VOF) method to solve sloshing problem in a rectangular tank. Navier-Stokes equations are solved by using an implicit time scheme finite volume method, an explicit time split scheme, which requires a small time step, is used for the volume fraction equation. In addition, our VOF method is able to preserve not only the volume but also remove the flotsam and jetsam problem.

Keywords and phrases: VOF method, interface, volume fraction.
Received March 31, 2014

1. Introduction

Sloshing is the periodic motion of the free surface of a liquid in partially tank. The inertial load exerted by the fluid is time-dependent and can be greater than the load exerted by a solid of the same mass. This makes analysis of sloshing especially important for transportation and storage tanks. Due to its dynamic nature, sloshing can strongly affect performance and behaviour of transportation vehicles, especially tankers filled with oil.

The problem of liquid sloshing in moving or stationary containers remains of great concern to aerospace, civil, and nuclear engineers, physicists, designers of road tankers and ship tankers. Civil engineers and seismologists have been studying liquid sloshing effects on large dams, oil tanks, and elevated water towers under ground motion. Since the early 1960s, the problem of liquid sloshing dynamics has been of major concern to aerospace engineers studying the influence of liquid propellant sloshing on the flight performance of jet vehicles. Large liquid movement creates highly localized impact pressure on tank walls, which may in turn cause structural damage and may even create sufficient moment to effect the stability of the vehicle, which carries the tank such in a tanker or spacecraft [1] and [2].

Sloshing is not a gentle phenomenon even at very small amplitude excitations. The fluid motion can become very non-linear, surface slopes can approach infinity and the fluid may encounter the tank top in an enclosed tanks. Hirt and Nichols [3] developed a method known as the volume of fluid (VOF). The flexibility of this method suggests that it could be applied to the numerical simulation of sloshing and is therefore used as a base in this study.

On the other hand, analytic results of sloshing problems are already found by many researchers. Some comprehensive reviews and discussions of the analytic and experimental studies of liquid sloshing are provided in

[4], [5], and [6]. The advent of high speed computers, the subsequent maturation of computational techniques for fluid dynamic problems and other limitations mentioned above have allowed a new, and powerful approach to sloshing; the numerical approach [7], [8], [9], and [10].

Numerical analysis of free surface (interface) fluid flow is a particularly difficult problem because the location of the free surface is unknown and has to be determined as part of the solution. One possible way to solve this problem is to linearize the free surface boundary conditions around a known base solution and introduce a perturbation due to the body and/or the waves. A review of linearization is presented in [11], [12], and [13]. However, in most codes for viscous flow, there are two broad approaches used, and following the nomenclature of Ferziger and Perić: interface tracking method and interface capturing methods.

In interface tracking methods (Lagrangian methods), the free surface is located at one boundary of the mesh, and the mesh deforms as the free surface moves. It is an explicit representative approach of the surface. They define the free surface as a sharp interface whose motion is followed. This approach includes the "*height function method*", where the free surface position is given by the values of a continuous function h, called *height function*, which is the distance between the free surface and a reference surface [11] and [14]. The principal limitation of Lagrangian methods is the inability to handle complex surface geometries and overturning waves.

Interface capturing methods are characterized by an *implicit representation* of the interface, which is tracked as part of the solution algorithm. The computations are performed on a fixed grid, which extends beyond the free surface. These methods are Marker-and-Cell method [15], [16], and [7]; Level-set method [19], [20], and [21]; Volume of fluid method [22], [23], [24], and [25]. They have a wide range of applications including problems in fluid mechanics, combustion, manufacturing of computer chips, computer animation, image processing, structure of snowflakes, the shape of soap bubbles, and satellite controllability. The main drawback of these methods is the possibility of numerical instability, diffusivity (with blurred interface).

The essential steps of the VOF interface method are as follows:

First, an initial prescribed interface topology is used to compute fluid volume fractions in each computational cell. This task requires the calculation of volumes truncated by the interface in each interface cell (partial filled cell). Exact interface information, is then discarded in favour of the discrete volume fraction data. Given a velocity field (provided by a flow solver), interfaces are then tracked by evolving fluid volumes in time with the solution of an advection equation. Typically, one can reconstruct the interface by the straightforward SLIC (simple line interface calculation) methods [26] and [27] or by various PLIC (piecewise linear interface calculation) methods [28], [29], [30], and [31]. The latter methods give much better results than the former, as noted in the review achieved by Kothe and Rider [32].

2. Numerical Formulation

2.1. Governing equations

The motion of the unsteady, viscous, incompressible two-phase flow is described by the Navier-Stokes equations:

- Continuity equation

$$\frac{\partial u_i}{\partial x_i} = 0. \tag{1}$$

- Momentum equations

$$\frac{\partial u_i}{\partial t} + \frac{\partial u_i u_j}{\partial x_j} = -\frac{1}{\rho}\frac{\partial p}{\partial x_i} + \frac{\partial}{\partial x_j}\left(\nu\left(\frac{\partial u_i}{\partial x_j} + \frac{\partial u_j}{\partial x_i}\right)\right) + g_i + \frac{f_i}{\rho}, \tag{2}$$

with

$$\rho = \rho_l + (1 - F)\rho_g,$$

$$\nu = \nu_l + (1 - F)\nu_g. \tag{3}$$

- Volume fraction equation

$$\frac{\partial F}{\partial t} + \frac{\partial F u_i}{\partial x_i} = 0. \tag{4}$$

In the above equations, u_i and g_i are the Cartesian velocity and the gravity components in i-direction, respectively, p is the pressure. ν_k and ρ_k are the viscosity and density, respectively, of the fluid k, where $k = g$ for gas and $k = l$ for liquid. The last term f_i is the surface tension force obtained via the continuum surface force (CSF) approach [33], which is active only on liquid-gas interface. The properties (density and viscosity coefficients) appearing in the momentum equation are determined by the presence of the component phase (volume fraction) F in each control volume, which is bounded by zero and one.

2.2. Discretisation

The finite volume discretisation of u_i-momentum equation is based on the integration over the control volume and time step. Quadratic upwind interpolation of convective kinetics (QUICK) scheme of Hayase et al. [34] is used for convective terms and central difference for diffusive terms and fully implicit time scheme. In order to avoid the numerical instability, often known as the "checkerboard problem", an improved Rhie-Chow interpolation [35] is used to calculate the convective flux. The spatial and temporal discretisation leads to the form of linear matrix equations as

$$Ax = b, \tag{5}$$

where

- A is the matrix obtained from discretisation of momentum.

- b is the vector which includes volume forces, extra terms of convective terms of high order, such as in TVD scheme [36] and [37].

- x is the unknown nodal velocity vector.

2.3. Interface modelling

The interface is treated as a shift in the fluid properties. Along the interface, the surface tension arises as the result of attractive forces between molecules in a fluid. Here, we use the continuum surface force (CSF) approach proposed in [33], which incorporates the surface tension as a volume force f_i included in the momentum equations

$$f_i = \sigma\kappa\nabla F_i, \tag{6}$$

where the curvature is (κ) defined by

$$\kappa = \nabla.\left(\frac{n}{|n|}\right) = \frac{1}{|n|}\left[\left(\frac{n}{|n|}.\nabla\right)|n| - \nabla.n\right], \tag{7}$$

where n is the interface normal vector defined by $n = \nabla F$.

Volume fractions transition abruptly across the interface, causing problem of accuracy when calculating the normal and the curvature. A solution to this problem is to first convolve F with a smooth kernel K to construct a smoothed or mollified function $\widetilde{F}$

$$\widetilde{F}(x) = k * F(x) = \int_\Omega F(x')K(x - x')dx' \approx \sum_\Omega F(x')K(x - x')\Delta x', \tag{8}$$

where Ω denotes the support of the kernel K (i.e., those points x for which $K(x) \neq 0$), which is typically compact (i.e., of finite extent).

Many types of kernels have been used in the past, such as Gaussians, B-spline, and polynomials. Some of these kernels are radially-symmetric while others are products of one-dimensional function. In this paper, we have chosen the Peskin function [38], which is given by

$$K(x - x_k) = \begin{cases} \prod_{n=1}^{\dim} \frac{1}{2d}\left(1 + \cos\frac{\pi(x_n - x_k)}{d}\right), & \text{if } |x - x_k| \leq d, \\ 0, & \text{otherwise}, \end{cases} \tag{9}$$

where dim is the partial dimension, $d = 2h$, with h the grid spacing, x is the grid coordinates, and x_k is the interface point coordinates. In this paper, the grid spacing is not uniform, so we have $h = \max(dx, dy)$.

2.4. Pressure correction simple method

The coupling between velocity and pressure is implicitly implemented by an auxiliary pressure correction equation. First, given a guessed pressure field, one can obtain a velocity field by solving momentum equations. This resulting velocity field may not satisfy the continuity equation. To enforce the continuity conservation, a correction procedure is needed. Then the pressure and velocities are corrected after solving pressure correction equation, which is obtained by substituting the assumed corrected velocities into continuity equation and integrating over the control volume.

2.5. Volume tracking algorithm

Piecewise linear interface calculation (PLIC) is one of the most widely employed geometric interface reconstruction scheme because of its accuracy, compared to the other methods, such as donor acceptor and Euler explicit method.

In PLIC method, the interface is approximated by a straight line of appropriate inclination in each cell. A typical reconstruction of the interface with a straight line in cell P, which yields an unambiguous solution, is perpendicular to an interface normal vector n_P and delimits a fluid volume matching the given F_P for the cell [40] and [41].

A cell-centred value of the normal vector n_P may be computed, as

$$n_P = \frac{n_{en} + n_{wn} + n_{es} + n_{ws}}{4}, \tag{10}$$

where $n_{en}, n_{wn}, n_{es},$ and n_{ws} are the normal vector estimated, respectively, at vertices east-north, west-north, east-south, and west-south of a rectangular cell with center P.

In PLIC method, the interface is approximated in each interface cell by a portion of a straight line in 2-D (plane in 3-D), defined by the equation

$$n_x x + n_y y = \lambda, \tag{11}$$

where λ is the interface constant (parameter which is related to the smallest distance between the interface and the origin); n_x and n_y are the Cartesian components of normal vector n_P. In each interface cell, the minimum between liquid volume V_l and gaz volume V_g is given by [42]

$$\min(V_l, V_g) = F_c dxdy = \frac{\lambda_c^2 - \max(0, (\lambda_c - dy_c)^2)}{2|n_x n_y|}, \tag{12}$$

where

$dx_1 = |n_x|dx$; $dy_1 = |n_y|dy$; $dx_c = \max(dx_1, dy_1)$; $dy_c = \min(dx_1, dy_1)$;

$\lambda_c = \min(\lambda, \lambda_m - \lambda)$; $\lambda_m = |n_x|dx + |n_y|dy = dx_1 + dy_1$; and

$F_c = \min(F, 1 - F)$.

2.5.1. Volume fluxes calculation

The flux estimation is based on the interface configuration inside the surface cell. The liquid volume δV, which flows through a face of a cell during a time step δt may be found using the interface parameter λ_c via the relation (12). For instance, the volume flux advected δV during time δt through the east face of the donor cell can be found as follows: Since the position of the interface is known in the donor cell, that is, λ_c is known, then we can apply relation (12) to the sub-region with lengths $dx - |u_e|\delta t$ and dy as shown by figure. From (12), we can write

$$F_c = \frac{\lambda_c^2 - \max(0, (\lambda_c - dy_c)^2)}{2dx_c dy_c}. \tag{13}$$

When $\lambda \leq 0.5\lambda_m$ and $n_x u_e < 0$

$$\delta V_e = F_D dxdy - F_c dy(dx - |u_e|\delta t). \quad (14)$$

When $\lambda > 0.5\lambda_m$ and $n_x u_e < 0$

$$\delta V_e = F_D dxdy - (1 - F_c)dy(dx - |u_e|\delta t). \quad (15)$$

When $\lambda \leq 0.5\lambda_m$ and $n_x u_e \geq 0$

$$\delta V_e = F_c dy|u_e|\delta t. \quad (16)$$

When $\lambda > 0.5\lambda_m$ and $n_x u_e \geq 0$

$$\delta V_e = (1 - F_c)dy|u_e|\delta t. \quad (17)$$

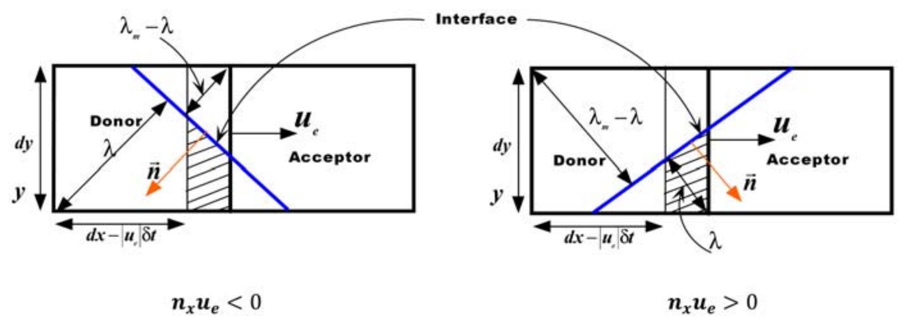

Figure 1. Calculation of the volume flux through the east-face (*e*) of the donor cell where liquid is under the interface.

Lagrangian approach is used in [43] to advance the old, reconstructed interface with interpolated velocities to a new position and the new Φ-field is deducted from the new interface locations. Here, we apply Eulerian techniques, which are mainly divided in two categories: multi-dimensional or unsplit schemes and one-dimensional or operator split schemes. Multi-dimensional schemes require only one reconstruction per time step, i.e., a full multi-dimensional solution is updated in a single time step. They are more complex because boundary fluxes depend on fluxes calculated along each coordinate direction. Examples of multi-dimensional algorithms can be found in [44]. Split schemes, on the other hand, construct the multi-dimensional solution as a series of sequential, one-dimensional sweeps.

$$\frac{F^{*} - F^{n}}{\Delta t} + \frac{\partial uF^{n}}{\partial x} = F^{*}\frac{\partial u}{\partial x}, \tag{18}$$

$$\frac{F^{n+1} - F^{*}}{\Delta t} + \frac{\partial vF^{*}}{\partial y} = F^{n}\frac{\partial v}{\partial y}, \tag{19}$$

where the advected volume fractions during a time step through east or west cell face (north or south) are given by

$$F_{e/w} = \frac{\delta V_{e/w}}{(|u|\delta t dy)_{e/w}}, \tag{20}$$

$$F_{n/s} = \frac{\delta V_{n/s}}{(|v|\delta t dx)_{n/s}}. \tag{21}$$

2.5.2. Coupling of implicit and explicit time methods

In this section, we propose our coupling method. Here, the momentum equations are solved implicitly. It is well known that time step for implicit scheme is unconstrained, that is, the scheme is unconditionally stable for reasonable large value of time step. In most of computational fluid codes, same time step is used to solve interface function equation, which may take too time to converge. In this paper, as well as in [45] and [46], a scheme in which the momentum equations are solved implicitly while interface equation is solved explicitly, so this means that , we use two different time steps such that

$$\delta t_i = k\delta t_e, \tag{22}$$

where k could be a relative large integer of order 1000; δt_i and δt_e are, respectively, in implicit and explicit time steps.

In the Figure 2(b), we can see that for one large time step to solve the momentum equations, the explicit time scheme used to solve the VOF method requires k loops. The main drawback of the implicit method is that it may take several minutes to converge over a loop. Although large time step can be used in implicit time scheme, the computational time would be too large when it is applied both for momentum and VOF equations. On the other hand, explicit time scheme requires no iteration, but time step must be relatively small in order to satisfy Courant-Friedrichs-Lewy criterion. That can lead to large computational time when both equations are solved by using explicit time scheme. In order to reduce computational time, we propose to combine the two schemes.

For the numerical results in this paper, several values of time steps as well as two-dimensional structured meshes have been tested. It is shown in this paper that using this new approach, the computational time is considerably reduced and the domain volume is conserved.

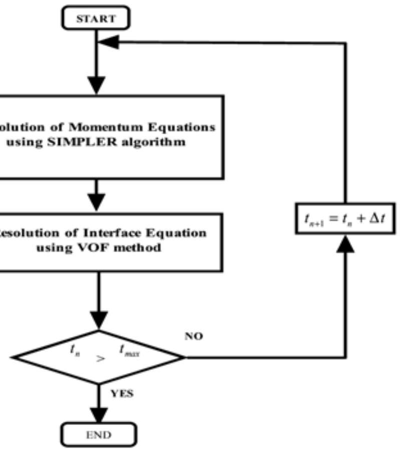

(a)

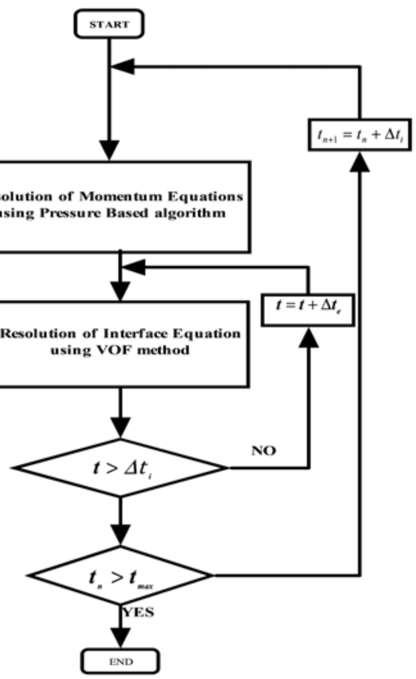

(b)

Figure 2. (a) Usual approach which uses the same time step both for all equations; (b) new implicit-explicit coupling method proposed here.

3. Numerical Results

Sloshing tank

The sloshing of the liquid can increase the dynamic pressure on the tank sides and bottom, so that the integrity of the tank is put at risk. An example is a ship carrying liquid cargo where sloshing can be critical in a partially filled tank. Another example is the case when the satellites start to accelerate for course corrections; the onboard fuel starts to slosh inducing a force and torque. This interaction between the motion of the satellite and the onboard sloshing liquid can have undesirable consequences as happened quite recently (1998) with NASA's Near Earth Asteroid Rendezvous (NEAR) craft, which was on its way to the asteroid 433 Eros, Jeroen Gerrrits [44]. In this test, a rectangular tank with fluid inside is initially at rest state. The tank is suddenly accelerated along the horizontal x-direction in a sinusoidal large-amplitude. The position of the tank is given by

$$x = A \sin\left(\frac{2\pi}{T} t\right) \text{ and } y = k = Cte. \tag{23}$$

The inertial body force is given by $F_i = -\rho V \ddot{x}$, where ρ is the density of the fluid, V is the volume of the liquid inside the control volume, and $\ddot{x}$ is the acceleration of the governing coordinate system, which is given by

$$\ddot{x} = -Aw^2 \sin\left(\frac{2\pi}{T} t\right). \tag{24}$$

Equation (2) includes inertial force caused by movement of liquid in the partially filled tank. We have

$$\frac{\partial u_i}{\partial t} + \frac{\partial u_i u_j}{\partial x_j} = -\frac{1}{\rho}\frac{\partial p}{\partial x_i} + \frac{\partial}{\partial x_j}\left(\nu\left(\frac{\partial u_i}{\partial x_j} + \frac{\partial u_j}{\partial x_i}\right)\right) + g_i + \frac{f_i}{\rho}, \tag{25}$$

where

$$f_i = (\ddot{x}, 0, 0). \tag{26}$$

For the first test, we have chosen $A = 0.1$ and $T = 2.5$.

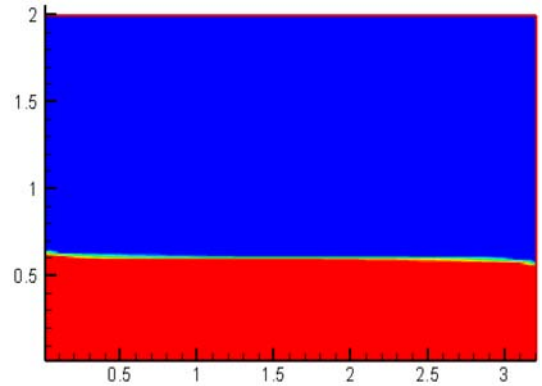

t=0.1 s

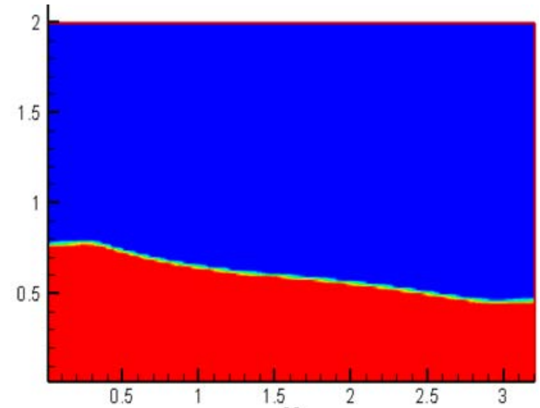

t=0.58 s

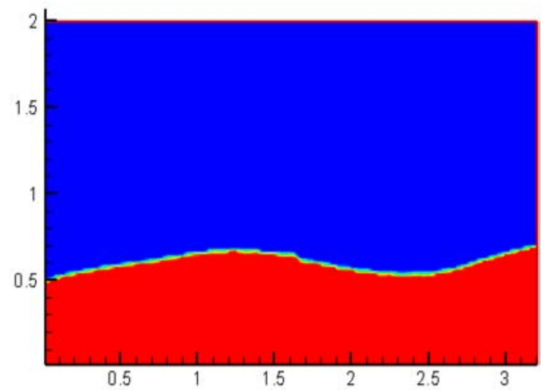

t=1.12 s

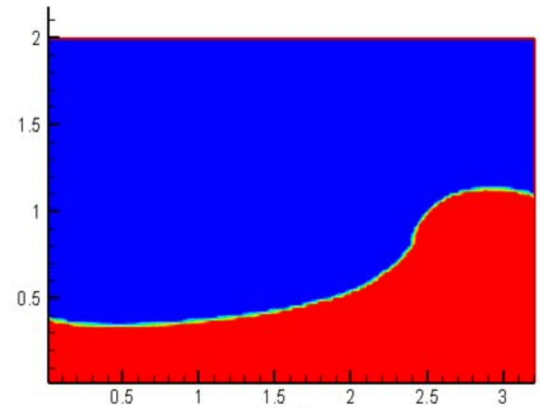

t=1.78 s

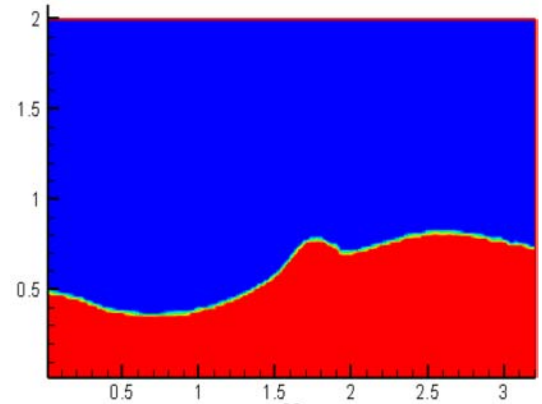

t=2.14 s

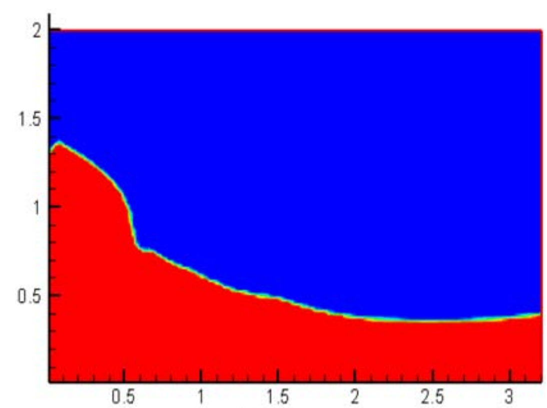

t=2.80 s

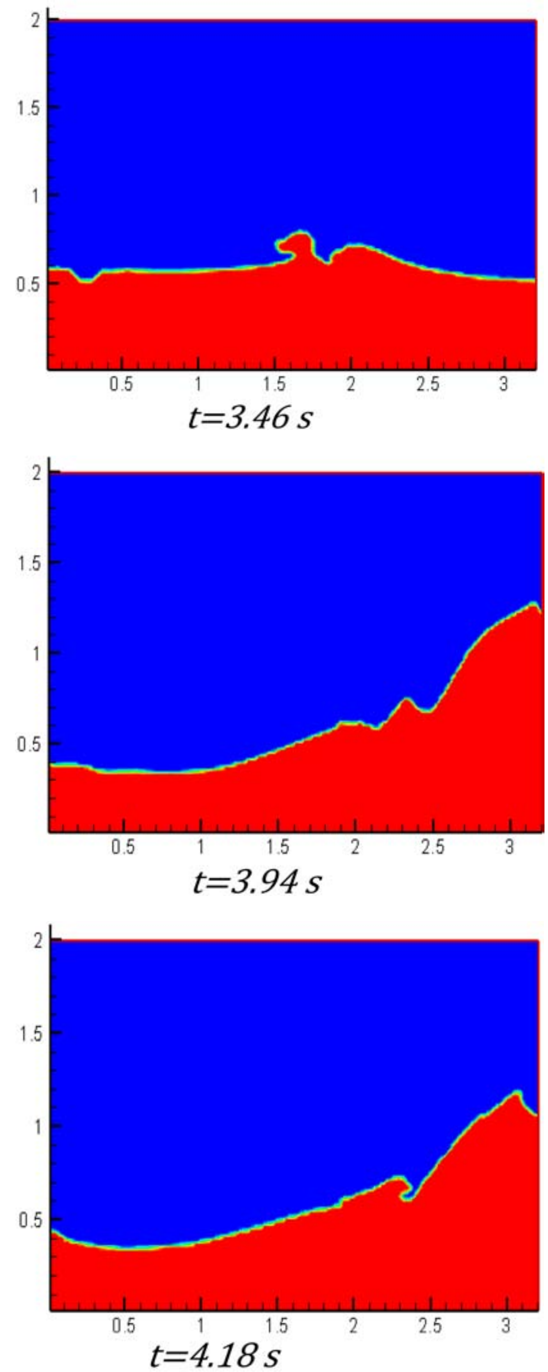
t=3.46 s
t=3.94 s
t=4.18 s

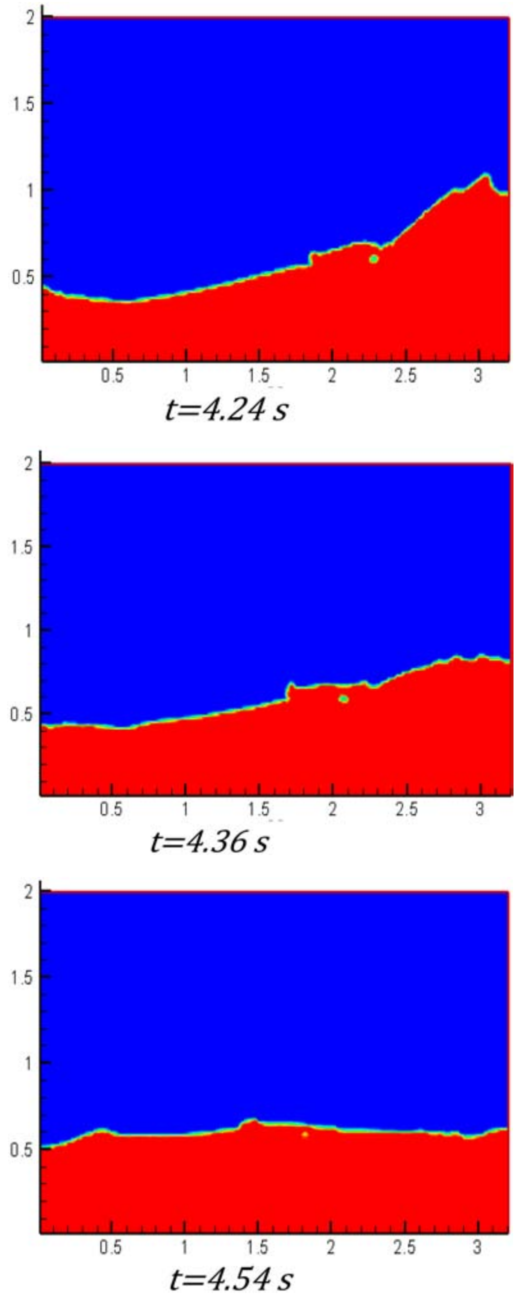

Figure 3. Free surface profile inside the tank submitted to horizontal oscillations with amplitude $A = 0.1\text{m}$ and period $T = 2.5\text{s}$.

Figure 3 describes the shape of the free surface inside a rectangular tank submitted to horizontal oscillations with amplitude $A = 0.1$m and period $T = 2.5$s.

When the tank starts to oscillate, from left to right, the liquid starts to flow from right to left due to inertia force. At time $t = 0.58$s, the direction of the flow is inverted, that is the first wave moves from left to right. At time $t = 1.12$s, a second wave moves in the same direction as the first one where they merge near the right wall, increasing the height on this wall at time $t = 1.78$s. This sloshing of the liquid inside the tank continues taking any arbitrary shape as shown in next instants.

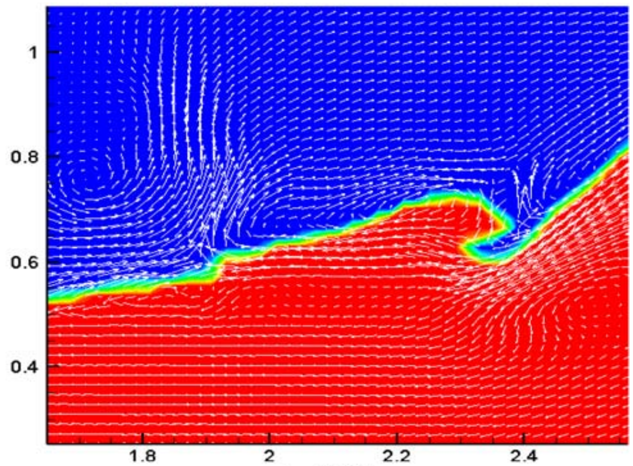

t=4.18s

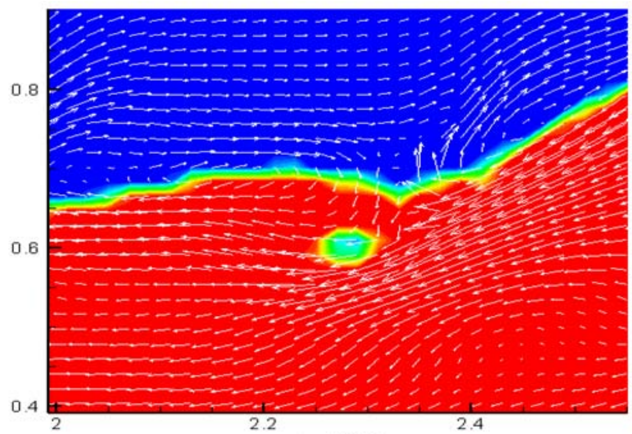

t=4.36s

Figure 4. Velocity field.

Velocity vectors near the interface are shown in Figure 4. At instant $t = 4.36\text{s}$, we can observe an air bubble. This is due to the fact that around this zone, some velocity vectors below are oriented to the left while some others above are directed to the right. The merging of these two flows gives the air bubble.

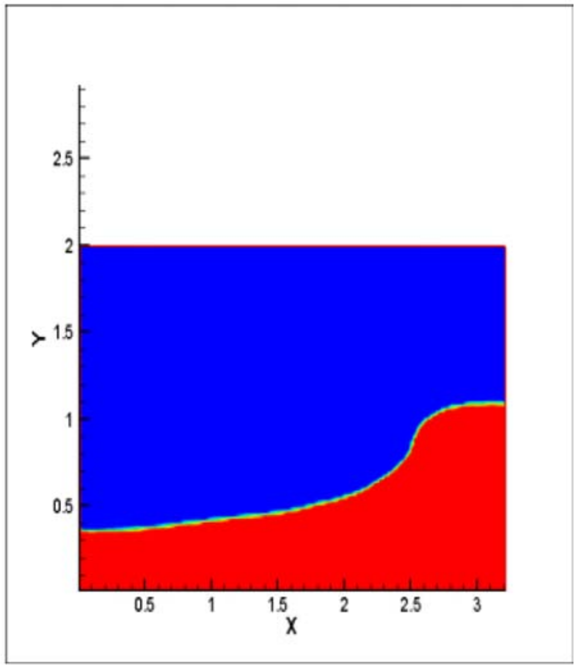

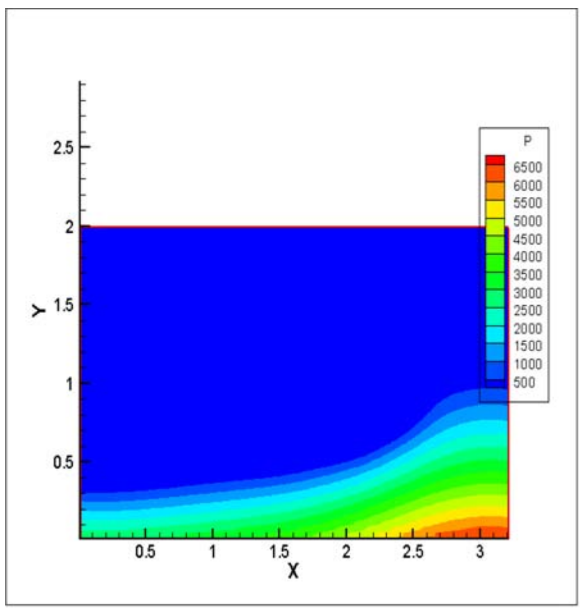

volume fraction $t = 1.6s$ *pressure*

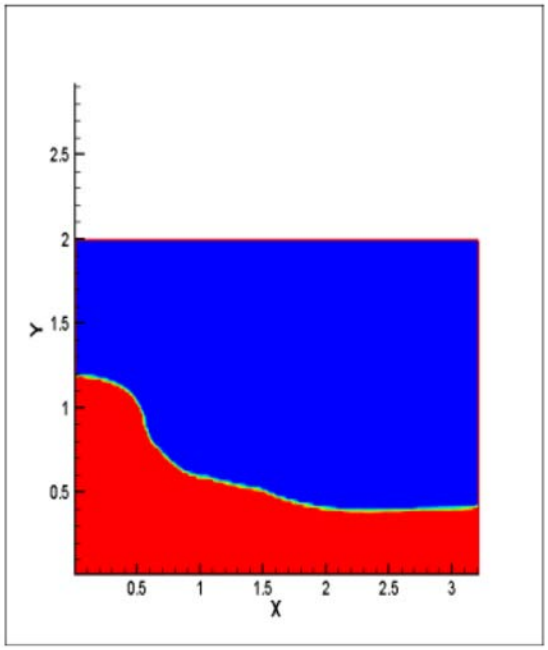

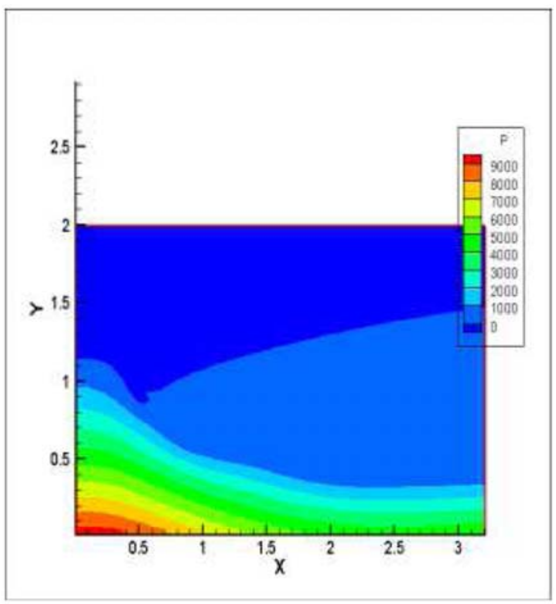

volume fraction $t = 2.68s$ *pressure*

Figure 5. Evolution of the interface due to horizontal excitation.

Pressure field on the bottom of the tank is shown in Figure 5. The pressure is greater on a corner when the mean wave collapses on the corresponding vertical side.

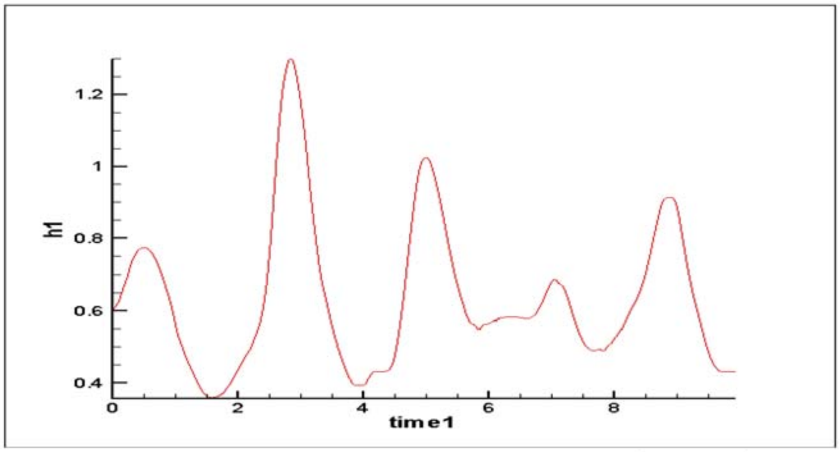

$$A = 0.2 \qquad T = 2.0 \qquad time1 = t * \sqrt{g / H}$$

Figure 6. Movement of the interface point along the right vertical wall.

Figure 6 shows height evolution of a free surface along the right wall. Initially the height is 0.6m. When the tank starts to oscillate horizontally from right to left, the liquid start to slosh from left to right due to inertial force, thus height increases. When the sloshing frequency approaches the tank frequency, the height along the wall becomes greater and vice versa.

In a next paper attention will be dedicated to this phenomena.

4. Conclusion

An implicit-explicit time scheme coupling has been presented and evaluated. The classical sloshing tank two-dimensional problem has been used to evaluate the computer code. The numerical results are shown to be in good agreement with other results reported in the open literature. It is shown that computational time is reduced with the coupling method.

References

[1] H. N. Abramson, Dynamic Behavior of Liquids in Moving Containers with Application to Space Vehicle Technology, NASA-SP-106, 1966.

[2] J. Gerrits, G. E. Loots, G. Fekken and A. E. P. Veldman, Liquid sloshing on earth and in space, in: Moving Boundaries V (B. Sarler, C. A. Brebbia and H. Power eds.), WIT Press, Southampton, (1999), pp. 111-120.

[3] C. W. Hirt and B. D. Nichols, Volume of fluid method for the dynamics of free boundaries, Journal of Computational Physics 39 (1981), 201-222.

[4] H. F. Bauer, C. D. Clark and J. H. Woodward, Analytical mechanical model for the description of the rotary propellant sloshing motion, Final Report, Contract NAS8-11159, Eng. Experiment Station, Georgia Tech., Atlanta, 1965.

[5] H. F. Bauer and J. Villenueva, Theory of liquid sloshing in a rectangular container with numerical examples for C-45A wing, Lockheed-Georgia Co., Rept. No ER 8390, 1966.

[6] O. M. Faltinsen, A non-linear theory of sloshing in rectangular tanks, J. of Ship Research 18(4) (1974), 224-241.

[7] O. M. Faltinsen, A numerical non-linear method of sloshing in tanks with two-dimensional flow, J. of Ship Research 22(3) (1978), 193-202.

[8] M. Arai, L. Y. Cheng and Y. Inoue, 3-D numerical simulation of impact load due to liquid cargo sloshing, Journal of the Society of Naval Architects of Japan 17(1) (1994).

[9] G. X. Wu, Q. W. Ma and R. E. Taylor, Numerical simulation of sloshing waves in a 3-D tank based on a finite element method, Applied Ocean Research 20 (1998).

[10] T. Nakayama and K. Washizu, Nonlinear analysis of liquid motion in a container subjected to forced pitching oscillation, Int. J. for Num. Meth. in Eng. 15 (1980), 1207-1220.

[11] J. N. Newmann, Linearized Wave Resistance Theory, International Seminar on Wave Resistance, Japan, 1976.

[12] H. C. Raven, Variation on a Theme by Dawson, Proceedings of the Seventeenth Symposium on Naval Hydrodynamics, The Hague.

[13] C. W. Dawson, A Practical Computer Method for Solving Ship-Wave Problems, 2nd International Conference on Numerical Ship Hydrodynamics, Berkeley, USA, 1977.

[14] J. L. Hess, Calculation of Potential Flow About Arbitrary Three-Dimensional Lifting Bodies, Douglas Report No. MDC J5679-01.

[15] Harlow and Welch, Numerical calculation of time dependent viscous incompressible flows of liquid with free surface, Phys. Fluids 8, 21-28.

[16] V. Armenio, An improved MAC method (SIMAC) for unsteady high-Reynolds free surface flows, Int. J. Numer. Methods Fluids 24 (1997), 185-214.

[17] D. Enright, R. Fedkiw and J. Mitchell, A hybrid particle level set method for improved interface capturing, J. Comput. Phys. 183 (2002), 83-116.

[18] Sebastien Tanguy and Alain Berlemon, Application of a level set method for simulation of droplet collisions, International Journal of Multiphase Flow 31 (2005), 1015-14035.

[19] Samuel Kokh, Gregoire Allaire and Sebastien Clerc, Towards Boiling Crisis Simulation: The Level-Set Method, Ninth International Topical Meeting on Nuclear Reactor Thermal Hydraulics, Oct. 3-8, 1999.

[20] S. Osher and R. P. Fedkiw, Level set methods: An overview and some recent results, J. Comput. Phys. 169 (2001), 463-502.

[21] M. Sussman, P. Smereka and S. Osher, Level set approach for computing solutions to incompressible two-phase flow, J. Comput. Phys. 114 (1994), 146-159.

[22] M. Sussman and E. G. Puckett, A coupled level set and volume-of fluid method for computing 3-D and axisymmetric incompressible two-phase flows, Journ. of Comput. Physical 162 (2000), 301-337.

[23] J. E. Pilliod Jr. and E. G. Puckett, Second order accurate volume-of-fluid algorithm for tracking material interfaces, J. Comp. Phys. 130 (1997), 269-682.

[24] K. Abe and K. Koro, A topology optimization approach using VOF method, Struct. Multidisc. Optim. 31 (2006), 470-479; DOI.10.1007/s00158-005-0582-5.

[25] D. Gueyffier, A. Nadim, J. Li, R. Scardovelli and S. Zaleski, Volume of fluid interface tracking with smoothed surface stress methods for three-dimensional flows, J. Comput. Phys. 152 (1999), 423-456.

[26] W. F. Noh and P. Woodward, SLIC (Simple Line Interface Calculation), Lecture Notes Physics, Springer, New York, 59 (1976), 330-340.

[27] Murray Rudman, Volume-tracking methods for interfacial flow calculations, International Journal for Numerical Methods in Fluids 24 (1997), 671-691.

[28] J. Longo, H. P. Huang and F. Stern, Solid-free surface juncture boundary layer and wake, Experiments in Fluids 25(4) (1998), 283-297.

[29] D. B. Kothe, W. J. Mosso and J. S. Brock, Volume tracking of interfaces having surface tension in two and three dimensions, AIAA 96, No. 0859.

[30] D. B. Kothe, M. W. Williams, K. L. Lam, D. R. Kozekwa, P. K. Tubesing and E. G. Puckett, A second-order accurate, linearity-preserving volume tracking algorithm for free surface flows on 3-D unstructured meshes, Proceedings of the 3rd ASME/JSME Joint Fluids Engineering Conference, San Francisco, California, USA, July 18-22, 1999.

[31] D. Gueyffier, A. Nadim, J. Li, R. Scardovelli and S. Zaleski, Volume of fluid interface tracking with smoothed surface stress methods for three-dimensional flows, J. Comput. Phys. 152 (1999), 423-456.

[32] D. B. Kothe and W. J. Rider, Reconstructing volume tracking, Journal of Comput. Phys. 141 (1998), 112-152. U.S. Department of Energy by Los Alamos National Laboratory.

[33] J. Brackbill, D. Kothe and C. Zemach, A continuum method for modelling surface tension, J. Comp. Phys. 100 (1992), 335-354.

[34] T. Hayase, J. A. C. Humphrey and R. Greif, A consistently formulated QUICK scheme for fast and stable convergence using finite volume iterative calculation procedures, J. Comput. Phys. 98(1) (1992), 108-118.

[35] S. Majumdar, Role of underrelaxation in momentum interpolation for calculation of flow with non-staggered grids, Numerical Heat Transfer 13 (1998), 125-132.

[36] Stanley Osher and Sukumar Chakravarthy, Very High Accurate TVD Schemes, Institute for Computer Applications in Sciences and Engineering NASA Langley Research Center, Hampton, Virginia 23665, Report No. 84-44.

[37] S. R. Chakravarthy and S. Osher, High resolution application of the Osher upwind scheme for the Euler equation, AIAA Paper 83-1943.

[38] C. S. Peskin, Numerical analysis of blood flow in the heart, J. Computational Phys. 25 (1977), 220-252.

[39] D. B. Kothe, W. J. Mosso and J. S. Brock, Volume tracking of interfaces having surface tension in two and three dimensions, AIAA 96, No. 0859.

[40] D. J. E. Harvie and D. F. Fletcher, A new volume of fluid advection algorithm: The stream scheme, Journal of Computational Physics 162 (2000), 1-32.

[41] Gihun Son, Efficient implementation of a coupled level-set and volume-of-fluid method for three-dimensional incompressible two-phase flows, Numerical Heat Transfer, Part B 43 (2003), 549-565.

[42] D. Gueyffier, A. Nadim, J. Li, R. Scardovelli and S. Zaleski, Volume of fluid interface tracking with smoothed surface stress methods for three-dimensional flows, J. Comput. Phys. 152 (1999), 423-456.

[43] J. E. Pilliod Jr. and E. G. Puckett, Second order accurate volume-of-fluid algorithm for tracking material interfaces, Technical Report, Lawrence Berkeley National Laboratory, 1997. No. LBNL-40744, Also Submitted to J. Computational Physics.

[44] Jeroen Gerrits and Arthur E. P. Veldam, Numerical simulation of coupled liquid-solid dynamics, Proceeding of European Congress on Computational Methods in Applied Sciences and Engineering, 2000.

[45] N. Coulibaly, H. Andre and J. J. Marchal, Coupling of implicit-explicit methods for two-phase flow with a fully volume preserving method, International Conference on Marine Research and Transportation, 2007.

[46] N. Coulibaly and A. Nguessan, Numerical simulation of the droplet impact on a surface using volume-of-fluid (VOF) method, Far East Journal of Applied Mathematics 39(1) (2010), 23-36.

[47] G. C. Feng, Dynamic loads due to moving liquid, AIAA Paper No. 73-409 (1973).

[48] O. M. Faltinsen, A numerical nonlinear method of sloshing in tanks with two-dimensional flow, J. of Ship Research 22(3) (1978), 193-202.

[49] D. Y. Lee and H. S. Choi, Study on sloshing in cargo tanks including hydro elastic effects, J. of Mar. Sci. Technology 4(1) (1999).

■